

A Gas Kinetic Scheme for the Simulation of Compressible Multicomponent Flows

Liang Pan^{1,3}, Guiping Zhao⁴, Baolin Tian^{1,2} and Shuanghu Wang^{1,2,*}

¹ Institute of Applied Physics and Computational Mathematics, Beijing 100088, China.

² Key Laboratory of Computational Physics, Institute of Applied Physics and Computational Mathematics, Beijing 100088, China.

³ The Graduate School of China Academy of Engineering Physics, Beijing 100088, China.

⁴ National Natural Science Foundation of China, Beijing 100085, China.

Received 28 March 2012; Accepted (in revised version) 21 March 2013

Communicated by Kun Xu

Available online 5 July 2013

Abstract. In this paper, a gas kinetic scheme for the compressible multicomponent flows is presented by making use of two-species BGK model in [A. D. Kotelnikov and D. C. Montgomery, A Kinetic Method for Computing Inhomogeneous Fluid Behavior, J. Comput. Phys. 134 (1997) 364-388]. Different from the conventional BGK model, the collisions between different species are taken into consideration. Based on the Chapman-Enskog expansion, the corresponding macroscopic equations are derived from this two-species model. Because of the relaxation terms in the governing equations, the method of operator splitting is applied. In the hyperbolic part, the integral solutions of the BGK equations are used to construct the numerical fluxes at the cell interface in the framework of finite volume method. Numerical tests are presented in this paper to validate the current approach for the compressible multicomponent flows. The theoretical analysis on the spurious oscillations at the interface is also presented.

AMS subject classifications: 76T10, 76P05, 76N15

Key words: Multicomponent flows, two-species BGK model, Chapman-Enskog expansion, gas kinetic scheme.

1 Introduction

The numerical methods for the compressible multicomponent flows have become important topics in the research of computational fluid dynamics. Over the past decades,

*Corresponding author. *Email addresses:* panliangjlu@sina.com (L. Pan), zhaogp@nsfc.gov.cn (G. Zhao), tian.baolin@iapcm.ac.cn (B. Tian), wang_shuanghu@iapcm.ac.cn (S. Wang)

significant progresses have been made to handle the multicomponent flows which are associated with discontinuities and shock waves. One of the popular approaches is to solve an extended system in which additional conservation equations are introduced to the original Euler equations. The additional equations describe the conservation of parameters, such as level set functions, mass fraction and ratio of specific heats in the mixture [1, 6, 13, 16, 21]. In order to eliminate the spurious oscillations and other computational inaccuracies in the conservative methods [1, 2, 11], some non-conservative approaches which capture the contact discontinuous by making use of additional non-conservative governing equations were proposed [1, 2, 11, 18–20, 22]. Another approach introduced by Karni [12] was to solve the Euler equations separately on each side of the interface by a method designed for a single-component flow, while the interface was dealt with in a different manner using a pressure evolution equation derived from the energy equation. Despite the fact that the method is not exactly conservative at the interface, reasonable results can be also obtained.

In recent years, the gas kinetic scheme based on the BGK model [3–5] for the compressible fluids proposed in [24,25] has attracted much attention. Based on the Chapman-Enskog expansion, the Euler as well as Navier-Stokes equations can be derived from the gas kinetic BGK model. In the framework of finite volume method, the BGK scheme makes use of the local integral solution of BGK model to compute a time-dependent gas distribution function at a cell interface. The numerical fluxes are obtained by taking moments of the distribution function in the gas evolution stage. As the BGK model is a statistical model, the particle transports and collisions are coupled in the whole gas evolution process, and the particle collision time controls the physical dissipative coefficients in the macroscopic equations. Since the gas evolution is associated with a relaxation process, i.e. from a non-equilibrium state to an equilibrium one, the entropy condition is satisfied automatically. Once the physical structure can be well resolved by the numerical cell size, in smooth regions, the scheme automatically gives an accurate compressible Navier-Stokes solution. Meanwhile, in the discontinuous regions, because of the delicate dissipative mechanism, the BGK scheme generates a stable and crisp shock transition. The BGK scheme has been extended to magnetohydrodynamics [23,28], hyperbolic conservation laws with source terms [24] and shallow water flow [30]. The high order BGK scheme has also been developed [14,27]. Recently, a unified gas kinetic scheme [29] is developed for all Knudsen number flows, which is an extension of the gas-kinetic scheme from the continuum flow to the rarefied regime with discretization of velocity space.

The BGK-Based numerical methods for the multicomponent flow have also been proposed in recent years. A gas kinetic scheme for multicomponent flow was presented in [15, 26]. The basic idea of this method is that the evolution of each component is governed by a BGK model with its own equilibrium state, and the equilibrium states of both components are coupled in space and time due to the course of particle collisions, and the common variables in the equilibrium states are the macroscopic velocities and temperatures. By incorporating a conservative γ -model proposed in [1] into the BGK scheme, a gas kinetic γ -model BGK scheme for the compressible multicomponent flow

was proposed in [8,9]. In the view of recovering the original equations by using the local equilibrium states, the γ -model equation in the conservation form can be easily incorporated into the BGK scheme. In this method, the interface of two materials with different ratios of specific heat is considered to be a contact discontinuity. Since only one BGK-model needs to be solved, the γ -model BGK scheme is computationally efficient than the scheme presented in [15,26].

The two-species BGK model was taken into consideration in [10]. In this model, the collisions between different species were taken into account. Similar with the methods proposed in [15,26], in this model, each species is treated separately. Since the collisions between different species are considered, more physical information could be obtained from this model. With the Chapman-Enskog expansion, the macroscopic governing equations can be derived. Compared with the conventional Euler and Navier-Stokes equations, the relaxation terms appear in the governing equations, which are derived from integral over the additional collision terms. A gas kinetic scheme for the multicomponent flow was presented based on this model. Because of the relaxation terms, the method of operator splitting is used so as to avoid the difficulty to deal with relaxation terms. Making use of a switch function which connects both continuous region and discontinuous region, the distribution functions were constructed at the cell interface, and numerical fluxes can be obtained by taking moments of the distribution functions.

In this paper, a gas kinetic scheme for the compressible multicomponent flows will be presented based on the two-species BGK model. With the Chapman-Enskog expansion, the governing equations derived in [10] will be presented. Similar with the Boltzmann equation and the conventional BGK model, the entropy condition of this two-species BGK model will be proved. Because both species are treated separately in the two-species BGK model, it is possible for us to obtain more information of each species. Because of the appearance of relaxation term, the method of operator splitting is also used. In the hyperbolic part, based on the integral solution of the two-species BGK model, we construct the distribution functions by solving the BGK equations. The numerical fluxes across the cell interface are obtained by taking moments of the distribution functions. In the relaxation part, the second order Runge-Kutta method is used to deal with the relaxation terms. The numerical experiments will be presented to validate the scheme in one and two dimensional cases. In the numerical results, the spurious oscillations are observed at the interface in the contour of velocity and pressure. Based on the initial conditions with a density discontinuity evolving with uniform pressure and velocity [1], we analyze the reason of spurious oscillations and obtain so-called moment conditions that should be satisfied at the interface. These conditions are criterions to construct kinetic-based scheme for the multicomponent flow.

This paper is organized as follows. In section 2, we will introduce the two-species BGK model, prove the entropy condition of this model, and derive the macroscopic governing equations with the Chapman-Enskog expansion. In section 3, the outline of the numerical scheme will be presented. In section 4, some one and two dimensional numerical examples are presented to validate the scheme. In section 5, the reason of the spurious

oscillations in the contour of velocity and pressure at the interface will be analyzed. The last section is the conclusion.

2 Two-species BGK model

2.1 BGK equations

In this paper, we consider two types of molecules, identified by 1 and 2, respectively, whose distribution functions f_1 and f_2 are functions of spatial coordinate \mathbf{x} , velocity-space coordinate \mathbf{v} and time t . The kinetic equations for each species are expressed as

$$\frac{\partial f_1}{\partial t} + \mathbf{v} \cdot \frac{\partial f_1}{\partial \mathbf{x}} = St(f_1), \quad (2.1)$$

$$\frac{\partial f_2}{\partial t} + \mathbf{v} \cdot \frac{\partial f_2}{\partial \mathbf{x}} = St(f_2), \quad (2.2)$$

where the collision terms $St(f_1)$ and $St(f_2)$ represent the time rate of change of f_1 and f_2 due to the collisions. If the collisions both between same species and different species are considered, the following collision terms are used

$$St(f_1) = -\frac{f_1 - g_1}{\tau_{11}} - \frac{f_1 - g_{12}}{\tau_{12}}, \quad (2.3)$$

$$St(f_2) = -\frac{f_2 - g_2}{\tau_{22}} - \frac{f_2 - g_{21}}{\tau_{21}}. \quad (2.4)$$

In the collision terms above, there are four collision times $\tau_{ij}, i, j = 1, 2$ to be specified. The four equilibrium states above are all local Maxwellian state

$$\begin{aligned} g_1(\mathbf{x}, \mathbf{v}, t) &= \rho_1 \left(\frac{\lambda_1}{\pi} \right)^{\frac{N_1+3}{2}} e^{-\lambda_1((\mathbf{v}-\mathbf{u}_1)^2 + \zeta_1^2)}, \\ g_{12}(\mathbf{x}, \mathbf{v}, t) &= \rho_1 \left(\frac{\tilde{\lambda}_1}{\pi} \right)^{\frac{N_1+3}{2}} e^{-\tilde{\lambda}_1((\mathbf{v}-\mathbf{u}_2)^2 + \zeta_1^2)}, \\ g_2(\mathbf{x}, \mathbf{v}, t) &= \rho_2 \left(\frac{\lambda_2}{\pi} \right)^{\frac{N_2+3}{2}} e^{-\lambda_2((\mathbf{v}-\mathbf{u}_2)^2 + \zeta_2^2)}, \\ g_{21}(\mathbf{x}, \mathbf{v}, t) &= \rho_2 \left(\frac{\tilde{\lambda}_2}{\pi} \right)^{\frac{N_2+3}{2}} e^{-\tilde{\lambda}_2((\mathbf{v}-\mathbf{u}_1)^2 + \zeta_2^2)}, \end{aligned}$$

where ρ_i is density, p_i is pressure and λ_i is function of density and pressure, with the relation $\lambda_i = \frac{\rho_i}{2p_i}$. $\zeta_i = (\zeta_i^1, \zeta_i^2, \dots, \zeta_i^{N_i})$ is the internal variables in N_i dimensions, and $(\zeta_i)^2 = (\zeta_i^1)^2 + \dots + (\zeta_i^{N_i})^2$. The ratio of specific heats for each species commonly denoted by γ_i which equals to $\frac{N_i+5}{N_i+3}$. $\mathbf{u}_i = (U_i, V_i, W_i)$ is the corresponding macroscopic flow velocity with three components in the x, y and z directions. $\tilde{\lambda}_i$ is an auxiliary macroscopic variable and should be chosen to make the conservation laws satisfied for the two-species system.

Similar with the conventional BGK model, the collision terms satisfy the compatibility conditions

$$\int (g_i - f_i) \psi_\alpha^i d\mathbf{v} d\zeta_i = 0, \tag{2.5}$$

where $\psi_\alpha^i = (1, \mathbf{v}, \frac{1}{2}(\mathbf{v}^2 + \zeta_i^2))$, $\alpha = 1, 2, 3$, $d\mathbf{v} d\zeta_i = du dv dw d\zeta_i^1 \dots d\zeta_i^{N_i}$, $i = 1, 2$.

Based on the gas kinetic theory, we have the following relation between the conservative variables $(\rho_i, \rho_i \mathbf{u}_i, \rho_i E_i)$ and the distribution function f_i for each species

$$\begin{aligned} \rho_i &= \rho_i(\mathbf{x}, t) = \int f_i d\mathbf{v} d\zeta_i, \\ \rho_i \mathbf{u}_i &= \rho_i \mathbf{u}_i(\mathbf{x}, t) = \int \mathbf{v} f_i d\mathbf{v} d\zeta_i, \\ \rho_i E_i &= \rho_i E_i(\mathbf{x}, t) = \int \frac{1}{2}(\mathbf{v}^2 + \zeta_i^2) f_i d\mathbf{v} d\zeta_i, \end{aligned}$$

where $\rho_i E_i$ is the total energy. The pressure tensor and heat flow vector are defined as

$$\begin{aligned} \Pi_i &= \int (\mathbf{v} - \mathbf{u}_i)(\mathbf{v} - \mathbf{u}_i) f_i d\mathbf{v} d\zeta_i, \\ \mathbf{q}_i &= \frac{1}{2} \int (\mathbf{v} - \mathbf{u}_i)((\mathbf{v} - \mathbf{u}_i)^2 + \zeta_i^2) f_i d\mathbf{v} d\zeta_i. \end{aligned}$$

In this model, there are $\tilde{\lambda}_i$ and τ_{ij} which need to be specified. In this paper, they are defined as follows

$$\tilde{\lambda}_1 = \tilde{\lambda}_2 = \tilde{\lambda} = \frac{(N_1 + 3) + (N_2 + 3)}{\frac{N_1 + 3}{\lambda_1} + \frac{N_2 + 3}{\lambda_2}}, \tag{2.6}$$

$$\frac{\rho_1}{\tau_{12}} = \frac{\rho_2}{\tau_{21}}. \tag{2.7}$$

In the conventional BGK model, the gas evolution is associated with a relaxation process i.e. from a non-equilibrium state f to an equilibrium state g . However, in this model, the collision terms describe the distribution function f_i evolves not only to the equilibrium state g_i , but also to an equilibrium state g_{ij} . Because of this relaxation process, the entropy condition is satisfied for the two-species BGK model. In the following subsections, the conservation laws and the entropy condition of the two-species BGK model will be proved.

2.2 Entropy condition

It is well-known that the Boltzmann equation and the conventional BGK model satisfy the entropy condition, i.e. H theorem [5, 24].

In this subsection, we will prove that, according to the conservative conditions Eqs. (2.6) and (2.7), the two-species BGK model Eqs. (2.1) and (2.2) also satisfy the entropy condition for the system.

First of all, let's define

$$H_i = \int f_i \ln f \, dv d\zeta_i,$$

$$F(H_i) = \int v f_i \ln f \, dv d\zeta_i,$$

as the entropy density and entropy flux. In order to prove the entropy condition, let's multiply $(1 + \ln f_i)$ on both sides of the two-species BGK model Eqs. (2.1), (2.2), and take integration with respect to $dv d\zeta_i$

$$\int \left(\frac{\partial f_i}{\partial t} + v \frac{\partial f_i}{\partial x} \right) (1 + \ln f_i) \, dv d\zeta_i = \int \left(\frac{g_i - f_i}{\tau_{ii}} + \frac{g_{ij} - f_i}{\tau_{ij}} \right) (1 + \ln f_i) \, dv d\zeta_i, \tag{2.8}$$

which gives

$$\frac{\partial H_i}{\partial t} + \nabla \cdot F(H_i) = \int \left(\frac{g_i - f_i}{\tau_{ii}} + \frac{g_{ij} - f_i}{\tau_{ij}} \right) (1 + \ln f_i) \, dv d\zeta_i.$$

Based on the compatibility conditions Eq. (2.5), for the first collision terms, we have

$$\int (g_i - f_i) (1 + \ln f_i) \, dv d\zeta_i = \int (g_i - f_i) (\ln f_i - \ln g_i) \, dv d\zeta_i \leq 0.$$

Meanwhile, according to the definition of g_{ij} and f_i , we have

$$\int (g_{ij} - f_i) \, dv d\zeta_i = 0.$$

Consequently, the additional collision terms could be written as follows

$$\begin{aligned} & \sum_{i=1}^2 \int \left(\frac{g_{ij} - f_i}{\tau_{ij}} \right) (1 + \ln f_i) \, dv d\zeta_i \\ &= \sum_{i=1}^2 \left(\int \left(\frac{g_{ij} - f_i}{\tau_{ij}} \right) (\ln f_i - \ln g_{ij}) \, dv d\zeta_i + \int \left(\frac{g_{ij} - f_i}{\tau_{ij}} \right) \ln g_{ij} \, dv d\zeta_i \right). \end{aligned}$$

The first term on the right side of the equation satisfy the following inequality

$$\sum_{i=1}^2 \int \left(\frac{g_{ij} - f_i}{\tau_{ij}} \right) (\ln f_i - \ln g_{ij}) \, dv d\zeta_i \leq 0.$$

According to the definition of the four equilibrium states, the relationship between the macroscopic variables and the distribution functions, and the conservative conditions Eqs. (2.6) and (2.7), the second term on the right side satisfies

$$\sum_{i=1}^2 \int \left(\frac{g_{ij} - f_i}{\tau_{ij}} \right) \ln g_{ij} \, dv d\zeta_i = -\tilde{\lambda} \frac{\rho_1}{\tau_{12}} (\mathbf{u}_1 - \mathbf{u}_2)^2 \leq 0.$$

Thus, the two-species BGK model satisfies the following inequality

$$\sum_{i=1}^2 \frac{\partial H_i}{\partial t} + \nabla \cdot \mathbf{F}(H_i) \leq 0. \quad (2.9)$$

Therefore, the two-species BGK model satisfy the entropy condition. The two-species system will evolve to equilibrium states due to particle collisions and the entropy condition guarantees the dissipative property in the two-species BGK system.

2.3 Chapman-Enskog expansion

Derivations of the Euler and Navier-Stokes equations from the Boltzmann equation can be found in [5]. And they can be also derived from BGK equation [4, 24]. In this section, we will present the corresponding ‘‘pseudo-Euler’’ equations and Navier-Stokes equations derived from the two-species BGK model in [10].

Multiplying Eqs. (2.1) and (2.2) by $\psi_\alpha^i = (1, \mathbf{v}, \frac{1}{2}(\mathbf{v}^2 + \xi_i^2))$, integrating and making use of the conservative conditions Eqs. (2.7) and (2.6), we obtain the following differential statement of the conservation laws for the whole two-species system

$$\frac{\partial \rho_i}{\partial t} + \frac{\partial}{\partial \mathbf{x}} \cdot \rho_i \mathbf{u}_i = 0, \quad (2.10a)$$

$$\frac{\partial \sum_i \rho_i \mathbf{u}_i}{\partial t} + \frac{\partial}{\partial \mathbf{x}} \cdot \sum_i (\rho_i \mathbf{u}_i \mathbf{u}_i + \Pi_i) = 0, \quad (2.10b)$$

$$\frac{\partial}{\partial t} \cdot \sum_i \frac{1}{2} \rho_i \left(\mathbf{u}_i^2 + \frac{N_i+3}{2\lambda_i} \right) + \frac{\partial}{\partial \mathbf{x}} \cdot \sum_i \left(\frac{1}{2} \rho_i \left(\mathbf{u}_i^2 + \frac{N_i+5}{2\lambda_i} \right) \mathbf{u}_i + \mathbf{u}_i \cdot \Pi_i + \mathbf{q}_i \right) = 0. \quad (2.10c)$$

These equations describe the conservation laws of the whole system.

By making using of the Chapman-Enskog expansion, the macroscopic equations for each species can be derived. For simplicity, in this subsection, we only present the corresponding equations for the zeroth and first order of the Chapman-Enskog expansion.

For the zeroth order Chapman-Enskog expansion, we have the following equations

$$\frac{\partial \rho_i}{\partial t} + \frac{\partial}{\partial \mathbf{x}} \cdot \rho_i \mathbf{u}_i = 0, \quad (2.11a)$$

$$\frac{\partial \rho_i \mathbf{u}_i}{\partial t} + \frac{\partial}{\partial \mathbf{x}} \cdot \rho_i \left(\mathbf{u}_i \mathbf{u}_i + \frac{1}{2\lambda_i} \right) = \frac{\rho_i}{\tau_{ij}} (\mathbf{u}_j - \mathbf{u}_i), \quad (2.11b)$$

$$\begin{aligned} \frac{\partial}{\partial t} \left(\frac{1}{2} \rho_i \left(\mathbf{u}_i^2 + \frac{N_i+3}{2\lambda_i} \right) \right) + \frac{\partial}{\partial \mathbf{x}} \cdot \frac{1}{2} \rho_i \left(\mathbf{u}_i^2 + \frac{N_i+5}{2\lambda_i} \right) \mathbf{u}_i \\ = \frac{\rho_i}{\tau_{ij}} \left(\frac{N_i+3}{2} \left(\frac{1}{2\lambda} - \frac{1}{2\lambda_i} \right) + \frac{\mathbf{u}_j^2 - \mathbf{u}_i^2}{2} \right). \end{aligned} \quad (2.11c)$$

These equations are so-called ‘‘pseudo-Euler’’ equations. Without the right-side relaxation terms, they are Euler equations for each species. The cross-species terms conserve

the total momentum and energy and will drive the velocities and temperatures of two species approach to the equilibration.

For the first order Chapman-Enskog expansion, we can get the corresponding Navier-Stokes equations

$$\frac{\partial \rho_i}{\partial t} + \frac{\partial}{\partial \mathbf{x}} \cdot \rho_i \mathbf{u}_i = 0, \tag{2.12a}$$

$$\frac{\partial \rho_i \mathbf{u}_i}{\partial t} + \frac{\partial}{\partial \mathbf{x}} \cdot \rho_i \left(\mathbf{u}_i \mathbf{u}_i + \frac{\mathbf{1}}{2\lambda_i} \right) = \frac{\rho_i}{\tau_{ij}} (\mathbf{u}_j - \mathbf{u}_i) - \frac{\partial}{\partial \mathbf{x}} \cdot \Delta \Pi_i, \tag{2.12b}$$

$$\begin{aligned} \frac{\partial}{\partial t} \cdot \frac{1}{2} \rho_i \left(\mathbf{u}_i^2 + \frac{N_i+3}{2\lambda_i} \right) + \frac{\partial}{\partial \mathbf{x}} \cdot \frac{1}{2} \rho_i \left(\mathbf{u}_i^2 + \frac{N_i+5}{2\lambda_i} \right) \mathbf{u}_i \\ = \frac{\rho_i}{\tau_{ij}} \left(\frac{N_i+3}{2} \left(\frac{1}{2\tilde{\lambda}} - \frac{1}{2\lambda_i} \right) + \frac{\mathbf{u}_j^2 - \mathbf{u}_i^2}{2} \right) - \frac{\partial}{\partial \mathbf{x}} \cdot \Delta \mathbf{q}_i. \end{aligned} \tag{2.12c}$$

The pressure tensor $\Delta \Pi_i$ and the heat flux vector $\Delta \mathbf{q}_i$ in Eq. (2.12) are defined as follows

$$\begin{aligned} \Delta \Pi_i &= -2\mu_i \left(\Lambda_i - \frac{1}{N_i+3} \mathbf{1} \frac{\partial}{\partial \mathbf{x}} \cdot \mathbf{u}_i \right) + \Delta \Pi_i^{cross}, \\ \Delta \mathbf{q}_i &= -\kappa_i \frac{\partial \Theta_i}{\partial \mathbf{x}} + \Delta \mathbf{q}_i^{cross}, \end{aligned}$$

where the viscosity is $\mu_i = \tau_{ii} \frac{\rho_i}{2\lambda_i}$, the thermal conductivity is $\kappa_i = \frac{N_i+5}{2} \tau_{ii} \frac{\rho_i}{2\lambda_i}$ and $\Theta_i = \frac{m_i}{2\lambda_i}$ where m_i is molecule mass. $\mathbf{1}$ is the unit symmetric tensor. Λ_i are the rate of strain tensor defined as follows

$$\Lambda_i = \frac{1}{2} \left(\frac{\partial \mathbf{u}_i}{\partial \mathbf{x}} + \widetilde{\frac{\partial \mathbf{u}_i}{\partial \mathbf{x}}} \right),$$

where the tilde is the transpose of the dyadic under it. The cross-species contributions to pressure tensor and heat flux are defined as

$$\begin{aligned} \Delta \Pi_i^{cross} &= \frac{\tau_{ii}}{\tau_{ij}} \left\{ (\mathbf{u}_i - \mathbf{u}_j)(\mathbf{u}_i - \mathbf{u}_j) - \frac{1}{N_i+3} \mathbf{1} (\mathbf{u}_i - \mathbf{u}_j)^2 \right\}, \\ \Delta \mathbf{q}_i^{cross} &= \frac{\tau_{ii}}{\tau_{ij}} \rho_i \left\{ \frac{N_i+5}{2} \left(\frac{1}{2\tilde{\lambda}} - \frac{1}{2\lambda_i} \right) (\mathbf{u}_i - \mathbf{u}_j) - \frac{1}{2} (\mathbf{u}_i - \mathbf{u}_j)(\mathbf{u}_i - \mathbf{u}_j)^2 \right\}. \end{aligned}$$

The above systems are closed with the equation of state (EOS) for each species. In order to avoid difficulties with thermodynamic modeling, in this paper, the ideal gas EOS is used

$$e_i = \frac{p_i}{\rho_i(\gamma_i - 1)}, \tag{2.13}$$

where γ_i are the ratio of the specific heats, $i = 1, 2$.

3 Numerical scheme

In the section above, we have proposed the two-species BGK model and discussed the relationship between the two-species model and macroscopic equations. In this section, we will present a gas kinetic scheme based on this model. First of all, the outline of the numerical methods will be given before we construct numerical scheme.

3.1 Outline of the numerical method

In this paper, we only consider the one dimensional case. Particularly, the directional splitting method is used in the two dimensional case. In this case, the two-species BGK model may be simplified as

$$\frac{\partial f_1}{\partial t} + u \frac{\partial f_1}{\partial x} = St(f_1), \tag{3.1}$$

$$\frac{\partial f_2}{\partial t} + u \frac{\partial f_2}{\partial x} = St(f_2), \tag{3.2}$$

where the collision terms $St(f_1)$ and $St(f_2)$ are defined in Eqs. (2.3) and (2.4) and the four equilibrium states are simplified as follows

$$\begin{aligned} g_1(x, u, t) &= \rho_1 \left(\frac{\lambda_1}{\pi}\right)^{\frac{K_1+1}{2}} e^{-\lambda_1(u-U_1)^2 + \tilde{\zeta}_1^2}, \\ g_{12}(x, u, t) &= \rho_1 \left(\frac{\tilde{\lambda}_1}{\pi}\right)^{\frac{K_1+1}{2}} e^{-\tilde{\lambda}_1(u-U_2)^2 + \tilde{\zeta}_1^2}, \\ g_2(x, u, t) &= \rho_2 \left(\frac{\lambda_2}{\pi}\right)^{\frac{K_2+1}{2}} e^{-\lambda_2((u-U_2)^2 + \tilde{\zeta}_2^2)}, \\ g_{21}(x, u, t) &= \rho_2 \left(\frac{\tilde{\lambda}_2}{\pi}\right)^{\frac{K_2+1}{2}} e^{-\tilde{\lambda}_2(u-U_1)^2 + \tilde{\zeta}_2^2}, \end{aligned}$$

where in one dimensional case, $K_i = N_i + 2$, $(\tilde{\zeta}_i)^2 = (\zeta_i^1)^2 + \dots + (\zeta_i^{N_i})^2 + v^2 + w^2$. U_i is the corresponding macroscopic flow velocity in the x direction. In the following section, for simplicity, denote $\tilde{\zeta}_i \triangleq \tilde{\zeta}_i$, $i = 1, 2$.

The corresponding macroscopic governing equations derived from the two-species BGK model in one dimensional case can be put into the following form

$$\frac{\partial \rho_i}{\partial t} + \frac{\partial}{\partial x} \cdot F_i^M = 0, \tag{3.3}$$

$$\frac{\partial \rho_i U_i}{\partial t} + \frac{\partial}{\partial x} \cdot F_i^P = \frac{\rho_i}{\tau_{ij}} (U_j - U_i), \tag{3.4}$$

$$\frac{\partial \rho_i E_i}{\partial t} + \frac{\partial}{\partial x} \cdot F_i^E = \frac{\rho_i}{\tau_{ij}} \left(\frac{K_i+1}{2} \left(\frac{1}{2\tilde{\lambda}} - \frac{1}{2\lambda_i} \right) + \frac{U_j^2 - U_i^2}{2} \right), \tag{3.5}$$

where the fluxes F_i^M, F_i^P and F_i^E can be defined as follows

$$\begin{pmatrix} F_i^M \\ F_i^P \\ F_i^E \end{pmatrix} = \int u \begin{pmatrix} 1 \\ u \\ \frac{1}{2}(u^2 + \zeta_i^2) \end{pmatrix} f_i dud\zeta_i,$$

where f_i is the distribution functions for each species, and $dud\zeta_i = dud\zeta_i^1 \dots d\zeta_i^{K_i}$.

Because of the relaxation terms in the equations above, the method of operator splitting has to be used, i.e. hyperbolic operator and relaxation operator.

A uniform mesh with $x_k = kh, (k=0,1,2,\dots)$ is considered, h is the mesh size and $x_{k+1/2}$ is the cell interface. The cell averaged mass, momentum, energy densities in the k -th cell in the n -th level each species are denoted by $W_k^{n,i}$. The solution is obtained by a succession of operators. For the second order scheme, we have:

$$W_k^{n+1,i} = L_s^{\Delta t/2} L_h^{\Delta t} L_s^{\Delta t/2} W_k^{n,i}, \tag{3.6}$$

where $L_h^{\Delta t}$ is the hyperbolic operator and $L_s^{\Delta t/2}$ is the relaxation operator.

3.2 Hyperbolic part

The hyperbolic part of Eqs. (3.3)-(3.5) could be written as

$$\frac{\partial \rho_i}{\partial t} + \frac{\partial}{\partial x} \cdot F_i^M = 0, \tag{3.7a}$$

$$\frac{\partial \rho_i U_i}{\partial t} + \frac{\partial}{\partial x} \cdot F_i^P = 0, \tag{3.7b}$$

$$\frac{\partial \rho_i E_i}{\partial t} + \frac{\partial}{\partial x} \cdot F_i^E = 0. \tag{3.7c}$$

In order to develop a conservative operator $L_h^{\Delta t}$, we integrate with respect $dxdt$ in $\Omega = [x_{k-1/2}, x_{k+1/2}] \times [t^n, t^{n+1}]$. Consequently, we have the following equation

$$W_k^{n+1,i} = W_k^{n,i} + \frac{1}{\Delta x} \int_{t^n}^{t^{n+1}} (F_{k-1/2}^i(t) - F_{k+1/2}^i(t)) dt, \tag{3.8}$$

where $F_{k+1/2}^i(t)$ is numerical flux of each phase at the cell interface and needs to be constructed for each species. By solving the two-species BGK equations, the distribution functions can be obtained at the cell interface. With the relationship between distribution functions and macroscopic variables, the numerical fluxes at the cell interfaces can be obtained by taking moments of the time-dependent gas distribution functions of each species.

For the BGK method, the reconstruction techniques are applied to the conservative variables directly. The cell averaged conservative variables in the k -th cell for each species

are denoted by W_k^i . The interpolated value in the k -th cell, is denoted by $\overline{W}_k^i(x)$. To second order accuracy, the interpolated value are written as

$$\overline{W}_k^i(x) = W_k^i + L(s_{k+}, s_{k-})(x - x_k),$$

where $x_{k-1/2} < x < x_{k+1/2}$. The nonlinear limiters are used in the construction of $L(s_{k+}, s_{k-})$, where $s_{k+} = (W_{k+1}^i - W_k^i)/h$ and $s_{k-} = (W_k^i - W_{k-1}^i)/h$. In this paper, Van Leer limiter is used.

If τ_{ij} is local constant, denote

$$\tau_i^* = \frac{\tau_{ii}\tau_{ij}}{\tau_{ii} + \tau_{ij}}, \quad x' = x_{k+1/2} - u(t - t'),$$

the integral solutions of Eqs. (3.1) and (3.2) at the cell interface $x = x_{k+1/2}$ may be written in the following form

$$f_i(x_{k+1/2}, t, u, \xi_i) = \int_0^t \left(\frac{g_i}{\tau_{ii}} + \frac{g_{ij}}{\tau_{ij}} \right) (x', t', u, \xi_i) e^{-(t-t')/\tau_i^*} dt' + e^{-t/\tau_i^*} f_i^0(x_{k+1/2} - ut), \quad (3.9)$$

where f_i^0 is the real gas distribution functions of f_i at the beginning of each time step $t = 0$, and g_i and g_{ij} are the corresponding equilibrium states. In order to obtain f_i , all these functions need be specified in the gas evolution stage.

For the second order accuracy, f_i^0 , g_i and g_{ij} around the interface $x_{k+1/2}$ can be constructed as

$$\begin{aligned} f_i^0 &= g_i^l (1 - H(x - x_{k+1/2})) (1 + a_i^l(x - x_{k+1/2})) + g_i^r H(x - x_{k+1/2}) (1 + a_i^r(x - x_{k+1/2})), \\ g_i &= g_i^0 (1 + (1 - H(x - x_{k+1/2})) (\overline{a}_r^i(x - x_{k+1/2})) + H(x - x_{k+1/2}) (\overline{a}_l^i(x - x_{k+1/2}))), \\ g_{ij} &= g_{ij}^0 (1 + (1 - H(x - x_{k+1/2})) (\overline{b}_r^i(x - x_{k+1/2})) + H(x - x_{k+1/2}) (\overline{b}_l^i(x - x_{k+1/2}))), \end{aligned}$$

where g_i^l , g_i^r and g_i^0 , g_{ij}^0 are corresponding local Maxwellian distribution functions located to the left, to the right and in the middle of a cell interface

$$\begin{aligned} g_i^l &= \rho_i^l \left(\frac{\lambda_i^l}{\pi} \right)^{\frac{K_i+1}{2}} e^{-\lambda_i^l ((u - U_i^l)^2 + \xi_i^2)}, \\ g_i^r &= \rho_i^r \left(\frac{\lambda_i^r}{\pi} \right)^{\frac{K_i+1}{2}} e^{-\lambda_i^r ((u - U_i^r)^2 + \xi_i^2)}, \\ g_i^0 &= \rho_i^0 \left(\frac{\lambda_i^0}{\pi} \right)^{\frac{K_i+1}{2}} e^{-\lambda_i^0 ((u - U_i^0)^2 + \xi_i^2)}, \\ g_{ij}^0 &= \rho_i^0 \left(\frac{\tilde{\lambda}_i^0}{\pi} \right)^{\frac{K_i+1}{2}} e^{-\tilde{\lambda}_i^0 (u - U_i^0)^2 + \xi_i^2}, \end{aligned}$$

$a_r^i, a_l^i, \bar{a}_r^i, \bar{a}_l^i$ and \bar{b}_r^i, \bar{b}_l^i are the corresponding slopes and $H(x)$ is the Heaviside function. The dependence of those slopes on the particle velocities is obtained from the Taylor expansion of a Maxwellian and can be written into the following form

$$\begin{aligned} a_l^i &= a_{1l}^i + a_{2l}^i u + a_{3l}^i \frac{1}{2}(u^2 + \zeta_i^2), & a_r^i &= a_{1r}^i + a_{2r}^i u + a_{3r}^i \frac{1}{2}(u^2 + \zeta_i^2), \\ \bar{a}_l^i &= \bar{a}_{1l}^i + \bar{a}_{2l}^i u + \bar{a}_{3l}^i \frac{1}{2}(u^2 + \zeta_i^2), & \bar{a}_r^i &= \bar{a}_{1r}^i + \bar{a}_{2r}^i u + \bar{a}_{3r}^i \frac{1}{2}(u^2 + \zeta_i^2), \\ \bar{b}_l^i &= \bar{b}_{1l}^i + \bar{b}_{2l}^i u + \bar{b}_{3l}^i \frac{1}{2}(u^2 + \zeta_i^2), & \bar{b}_r^i &= \bar{b}_{1r}^i + \bar{b}_{2r}^i u + \bar{b}_{3r}^i \frac{1}{2}(u^2 + \zeta_i^2), \end{aligned}$$

where all the above coefficients in those slopes are local constants.

By using the relation between the slopes of macroscopic variables and distribution functions of each species on the left and right hand sides separately, we have

$$\int \psi_\alpha^i g_\alpha^l dud\zeta_i = \bar{W}_k^i(x_{k+1/2}), \quad \int \psi_\alpha^i g_\alpha^r dud\zeta_i = \bar{W}_{k+1}^i(x_{k+1/2}).$$

The slopes a_l^i and a_r^i can be computed from

$$\int \psi_\alpha^i a_l^i g_\alpha^l dud\zeta_i = \frac{2(\bar{W}_k^i(x_{k+1/2}) - W_k^i)}{h}, \quad \int \psi_\alpha^i a_r^i g_\alpha^r dud\zeta_i = \frac{2(W_{k+1}^i - \bar{W}_{k+1}^i(x_{k+1/2}))}{h},$$

where the similar solution of a_l^i and a_r^i can be found in [24, 25].

After the initial state f_0^i is constructed, the equilibrium state g_0^i located at interface can be determined through the compatibility condition (2.5)

$$\begin{aligned} \int \int_{-\infty}^{+\infty} \psi_\alpha^i g_\alpha^0 dud\zeta_i &= \int \int \psi_\alpha^i f_0^i(-ut) dud\zeta_i \\ &= \int \int_{u>0} \psi_\alpha^i g_\alpha^l dud\zeta_i + \int \int_{u<0} \psi_\alpha^i g_\alpha^r dud\zeta_i. \end{aligned}$$

According to the definition of g_0^i , the conservative variables at the interface, which is denoted as W_0^i , could be constructed.

Similarly, the slopes \bar{a}_l^i and \bar{a}_r^i in g_i could also be obtained from the relationship between distribution function and macroscopic variables

$$\int \psi_\alpha^i \bar{a}_l^i g_\alpha^0 dud\zeta_i = \frac{2(W_0^i - W_k^i)}{h}, \quad \int \psi_\alpha^i \bar{a}_r^i g_\alpha^0 dud\zeta_i = \frac{2(W_{k+1}^i - W_0^i)}{h}.$$

Based on the definitions of four equilibrium states and W_0^i constructed above, we can construct the conservative variables corresponding to g_{ij}^0 at the cell interface can be constructed, denoted by \tilde{W}_{j0}^i , and the variable at the j th node corresponding to g_{ij} , which

is denoted by \tilde{W}_j^i . By making use of the relationship between distribution function and macroscopic variables, we have

$$\int \psi_\alpha^i \bar{b}_l^i g_{ij}^0 dud\zeta_i = \frac{2(\tilde{W}_0^i - \tilde{W}_k^i)}{h}, \quad \int \psi_\alpha^i \bar{b}_r^i g_{ij}^0 dud\zeta_i = \frac{2(\tilde{W}_{k+1}^i - \tilde{W}_0^i)}{h}.$$

The slope \bar{b}_l^i and \bar{b}_r^i can be computed by the same method introduced in [24, 25].

Substituting f_i^0 , g_i and g_{ij} into Eq. (3.9), the final gas distribution function at the cell interface can be expressed as

$$\begin{aligned} f_i = & (1 - e^{-t/\tau_i^*}) \tau_i^* \left(\frac{g_i^0}{\tau_{ii}} + \frac{g_{ij}^0}{\tau_{ij}} \right) \\ & + \left(-\tau_i^* + \tau_i^* e^{-t/\tau_i^*} + t e^{-t/\tau_i^*} \right) \frac{\tau_i^*}{\tau_{ii}} \left(\bar{a}_l^i H(u) + \bar{a}_r^i (1 - H(u)) \right) u g_i^0 \\ & + \left(-\tau_i^* + \tau_i^* e^{-t/\tau_i^*} + t e^{-t/\tau_i^*} \right) \frac{\tau_i^*}{\tau_{ij}} \left(\bar{b}_l^i H(u) + \bar{b}_r^i (1 - H(u)) \right) u g_{ij}^0 \\ & + e^{-t/\tau_i^*} \left((1 - ut a_l^i) H(u) g_i^l + (1 - ut a_r^i) (1 - H(u)) g_i^r \right). \end{aligned} \tag{3.10}$$

Finally, the numerical fluxes across the cell interface can be computed by taking moments of the distribution functions f_i for each species

$$F_{k+1/2}^i(t) = \int u \begin{pmatrix} 1 \\ u \\ \frac{1}{2}(u^2 + \zeta_i^2) \end{pmatrix} f_i dud\zeta_i, \tag{3.11}$$

with the numerical fluxes across the interface, Eq. (3.8) for each species can be updated inside each cell.

3.3 Relaxation part

In the previous subsections, the relaxation terms are not considered. In this subsection, we will deal with the relaxation part which describes the equilibration between each species

$$\frac{d}{dt} \rho_i U_i = \frac{\rho_i}{\tau_{ij}} (U_j - U_i), \tag{3.12}$$

$$\frac{d}{dt} \rho_i E_i = \frac{\rho_i}{\tau_{ij}} \left(\frac{N_i + 3}{2} \left(\frac{1}{2\tilde{\lambda}} - \frac{1}{2\lambda_i} \right) + \frac{U_j^2 - U_i^2}{2} \right). \tag{3.13}$$

As discussed in [10], the ordinary differential equations are analytically soluble in the time. But for simplicity, we make use of the second order Runge-Kutta method to deal

with the ordinary differential equations Eqs. (3.12) and (3.13). The time step is Δt , at $t=t^n$. From the conservative variables, $\rho_i^n, U_i^n, \lambda_i^n, i=1,2$ and $\tilde{\lambda}^n$ can be constructed. In the k -th cell, denote

$$\theta_{1,k}^i(\rho_i, U_i, U_j) = \left(\frac{\rho_i}{\tau_{ij}} (U_j - U_i) \right)_k,$$

$$\theta_{2,k}^i(\rho_i, U_i, U_j, \lambda_i, \tilde{\lambda}) = \left(\frac{\rho_i}{\tau_{ij}} \left(\frac{N_i + 3}{2} \left(\frac{1}{2\tilde{\lambda}} - \frac{1}{2\lambda_i} \right) + \frac{U_j^2 - U_i^2}{2} \right) \right)_k.$$

The intermediate conservative variables are updated,

$$(\rho_i U_i)_k^* = (\rho_i U_i)_k^n + \Delta t \theta_{1,k}^i(\rho_i^n, U_i^n, U_j^n),$$

$$(\rho_i E_i)_k^* = (\rho_i E_i)_k^n + \Delta t \theta_{2,k}^i(\rho_i^n, U_i^n, U_j^n, \lambda_i^n, \tilde{\lambda}^n).$$

Then we can get $(\rho_i^*)_k, (U_i^*)_k, (\lambda_i^*)_k, i=1,2$ and $(\tilde{\lambda}^*)_k$. Finally, we could obtain the conservative variables at $t^{n+1} = t^n + \Delta t$

$$(\rho_i U_i)_k^{n+1} = (\rho_i U_i)_k^n + \frac{\Delta t}{2} \left(\theta_{1,k}^i(\rho_i^n, U_i^n, U_j^n) + \theta_{1,k}^i(\rho_i^*, U_i^*, U_j^*) \right),$$

$$(\rho_i E_i)_k^{n+1} = (\rho_i E_i)_k^n + \frac{\Delta t}{2} \left(\theta_{2,k}^i(\rho_i^n, U_i^n, U_j^n, \lambda_i^n, \tilde{\lambda}^n) + \theta_{2,k}^i(\rho_i^*, U_i^*, U_j^*, \lambda_i^*, \tilde{\lambda}^*) \right).$$

During the equilibration process, we could observe that the total momentum and energy are conserved. However, in the region where $\tau_{ij} \sim \tau_{ji}$, the temperatures and velocities should be equilibrated instantly. Then the equilibration procedure may be simplified by calculating the velocity and temperature from the conservation requirements

$$\rho_1 U_1 + \rho_2 U_2 = (\rho_1 + \rho_2) U,$$

$$\frac{1}{2} \rho_1 \left(U_1^2 + \frac{3}{2\lambda_1} \right) + \frac{1}{2} \rho_2 \left(U_2^2 + \frac{3}{2\lambda_2} \right) = \frac{1}{2} (\rho_1 + \rho_2) \left(U^2 + \frac{3}{2\lambda} \right).$$

Then $(\rho_i U_i)_k^{n+1}$ and $(\rho_i E_i)_k^{n+1}$ could be updated by the above conservation requirements.

Thus we have constructed the relaxation operator $L_s^{\Delta t/2}$ for Eqs. (3.12) and (3.13).

4 Numerical experiments

In this section, we will test the proposed gas-kinetic numerical scheme on some well-known multicomponent flow applications such as the one-dimensional shock tube problem, the two-dimensional cylindrical shock wave implosion and the shock bubble interaction. These numerical examples, which have been tested in many papers, validate our algorithm for the numerical simulations of multicomponent flow. In the two-dimension case, the directional splitting method is used, and the method of solving the slope, which

could be found in [24]. The collision times are different in the hyperbolic and relaxation part.

In the hyperbolic part, the collision time τ is defined as

$$\tau = C_1 \Delta t + C_2 \left| \frac{p_l - p_r}{p_l + p_r} \right| \Delta t, \quad (4.1)$$

where the Δt is the time step, p_l and p_r are the corresponding total pressures of both species of the states g_l^i and g_r^i in the initial gas distribution function f_0^i . The first term on the right hand side gives a limiting threshold for the collision time to avoid the blowing up the program, it also provides a background dissipation for the numerical fluid. In the hyperbolic part, the jumps should be taken into account, so the second term in Eq. (4.1) is related to the pressure jump in the reconstructed initial data, which guarantees the real gas distribution function will stay on non-Maxwellian state in the non-equilibrium flow region.

In the relaxation part, for simplicity, the collision time could be defined as

$$\tau = \epsilon \Delta t. \quad (4.2)$$

The collision time between the same species τ_{ii} , $i=1,2$ are defined as

$$\tau_{ii} = \tau. \quad (4.3)$$

In order to satisfy the conservative condition Eqs. (2.6) and (2.7), the collision time between different species τ_{ij} , $i,j=1,2$ are defined as:

$$\tau_{ij} = \frac{\rho_i + \rho_j}{\rho_j} \tau, \quad (4.4)$$

In following test cases, $C_1 = 0.01$, $C_2 = 5$, in one dimensional cases $\epsilon = 15$ and in two dimensional cases $\epsilon = 30$ are used.

The two-fluid dynamics which we have derived reduces to the dynamics of a single-species fluid (say, species i) when the density of the other species (say, ρ_j) becomes very small in a region, relative to ρ_i . In this case, problems arise in calculating, for example, τ_{ij} and λ_j . To avoid the problem, in the calculation, we may set $\rho_j = 10^{-4} \sim 10^{-3}$ and $\lambda_j = 10$.

In the following numerical tests, the ideal gas EOS (2.13) is used in this paper.

4.1 Shock tube problems

The shock tube problems are presented to validate the current approach for multicomponent flow calculations.

- (1). The first case is Sod problem [11, 13, 24] and the initial condition is

$$\begin{aligned} (\rho, u, p, \gamma)_l &= (1, 0, 1, 5/3), \\ (\rho, u, p, \gamma)_r &= (0.125, 0, 0.1, 1.4). \end{aligned}$$

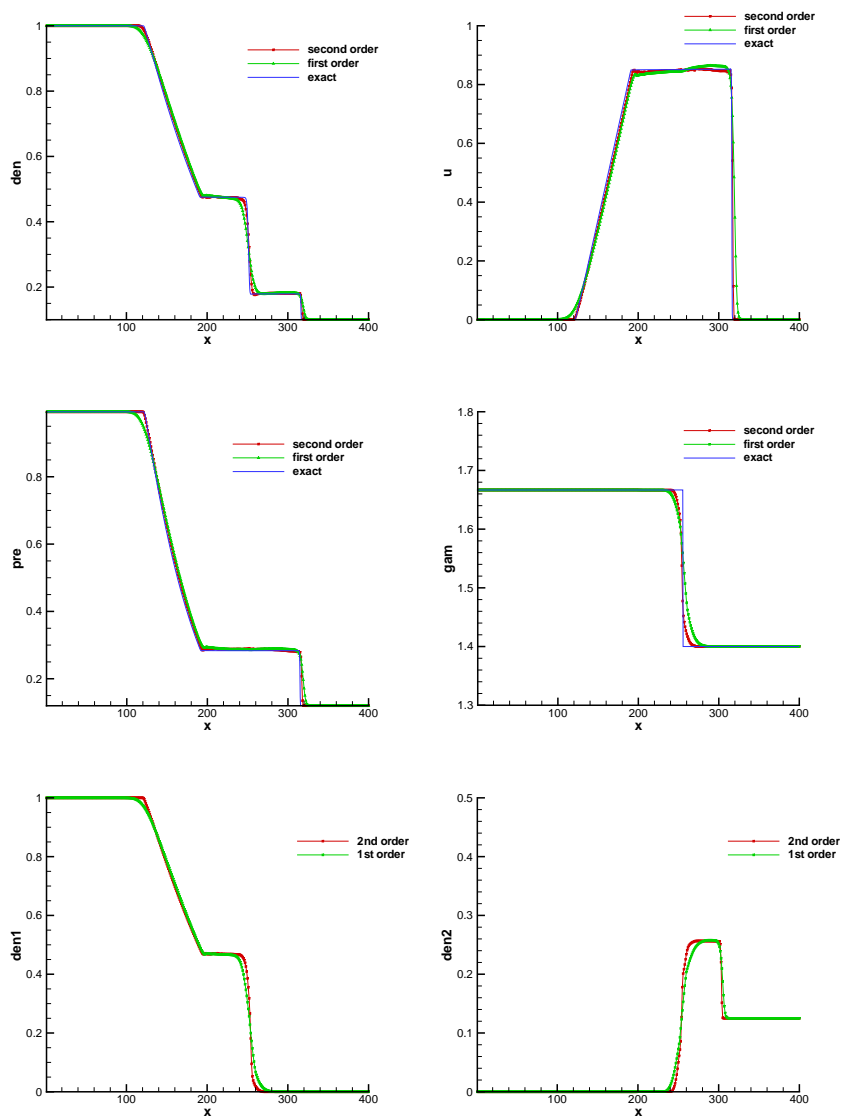


Figure 1: the numerical results of the first case of the shock tube problem.

(2). The second case is two rarefaction wave problem and initial condition is

$$\begin{aligned}
 (\rho, u, p, \gamma)_l &= (1, -1, 1, 5/3), \\
 (\rho, u, p, \gamma)_r &= (1, 1, 1, 1.4).
 \end{aligned}$$

In the calculations, the length of the numerical domain is equal to 400 and each cell size is $\Delta x = 1$. The van Leer's limiter is used in the scheme for the reconstruction of conservative

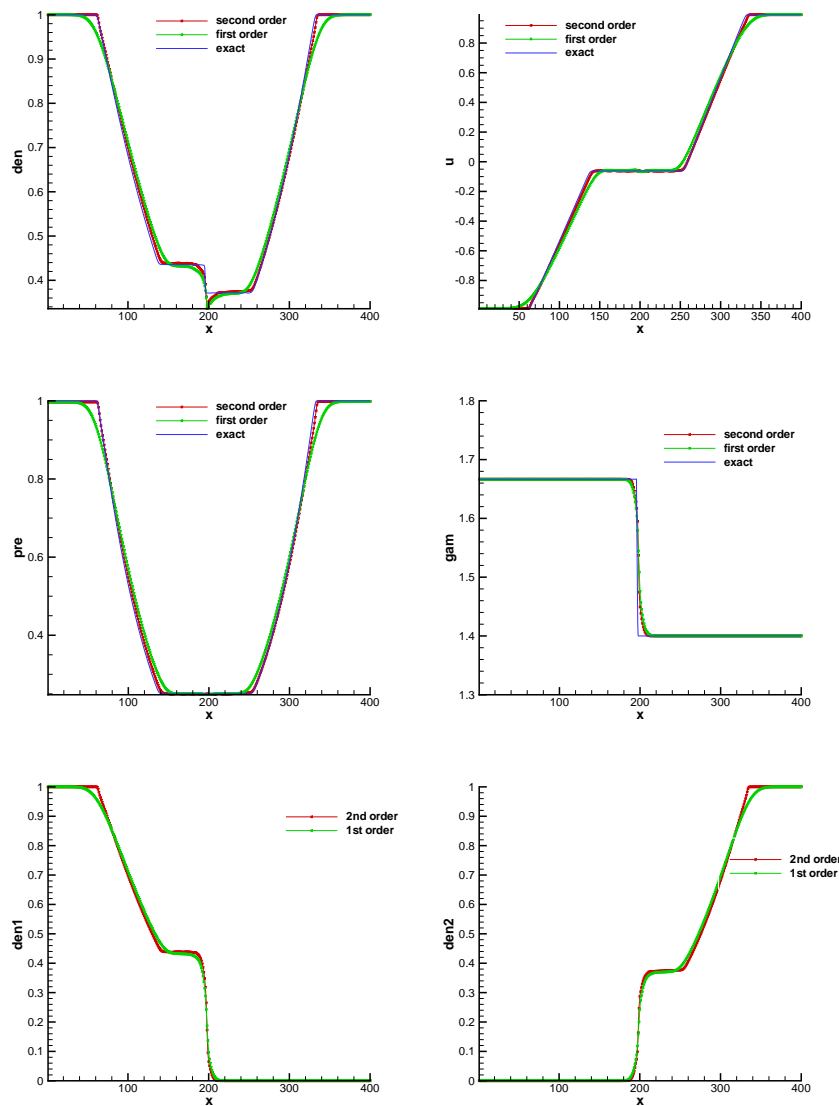


Figure 2: the numerical results of the second case of the shock tube problem.

variables for each component directly without imposing any specific numerical requirement for a smooth interface transition. The time step is determined by the common CFL condition where the CFL number is equal to 0.15. In the calculations, the initial discontinuities are located at $x=200$. The numerical solutions and exact solutions of the two tests are presented in Figs. 1 and 2 for the total density $\rho_1 + \rho_2$, average velocity $U = \frac{\rho_1 u_1 + \rho_2 u_2}{\rho_1 + \rho_2}$, total pressure $p = p_1 + p_2$, average ratio of specific heat $\gamma = \frac{\rho_1 \gamma_1 + \rho_2 \gamma_2}{\rho_1 + \rho_2}$ in each cell at $t = 60$. Moreover, the numerical results of individual mass densities ρ_1, ρ_2 for each component

in each cell at $t = 60$ are also presented. Here we could observe that the total density, velocity, pressure and average ratio of specific heat are generally in good agreement with the exact solution.

4.2 The shock bubble interaction

We consider the interaction of a Mach 1.22 shock wave with a helium cylindrical bubble [17]. Some theoretical analysis was presented in [31]. The problem was tested in the following two kinds of initial conditions:

- (1). The first kind of initial condition is

$$\begin{aligned} (\rho, u, v, p, \gamma) &= (1, 0, 0, 1, 1.4) && \text{Pre-shock,} \\ (\rho, u, v, p, \gamma) &= (1.3764, 0.394, 0, 1.5698, 1.4) && \text{Post-shock,} \\ (\rho, u, v, p, \gamma) &= (3.1358, 0, 0, 1, 1.285) && \text{Bubble.} \end{aligned}$$

- (2). The second kind of initial condition is

$$\begin{aligned} (\rho, u, v, p, \gamma) &= (1, 0, 0, 1, 1.4) && \text{Pre-shock,} \\ (\rho, u, v, p, \gamma) &= (1.3764, 0.394, 0, 1.5698, 1.4) && \text{Post-shock,} \\ (\rho, u, v, p, \gamma) &= (0.1358, 0, 0, 1, 1.67) && \text{Bubble.} \end{aligned}$$

In this test, on the up and lower boundary, the reflection boundary conditions are used in the two tests. In the calculations, 200×100 grids are used and each cell size is $\Delta x = 1$ and $\Delta y = 1$. The bubble is assumed in both thermal and mechanical equilibrium with the surrounding air. The diameter of the bubble is 19 cells. Initially, the shock is located at $x = 40$ and the center of bubble is at $(x, y) = (61, 50)$. CFL number equals to 0.15. The results are shown in Figs. 3 and 4 where contours of density are given at three different times. We could observe that the numerical results reproduce the large-scale structure of the corresponding numerical result in [6, 8] and of the experiments described in [7].

4.3 Cylindrical implosion

In this case, we consider the cylindrical implosion problem. A similar case was tested in [10] and some theoretical analysis was also presented in [31]. Initially, a cylindrical inner region with a lower density and lower pressure, the fluid is surrounded by the outer region with higher density and higher pressure fluid. The state evolves into an imploding shock inside the inner fluid and a rarefaction wave in the outer one. This test was performed on the two-dimensional domain of 200×200 cells of the size $\Delta x = \Delta y = 1$. The diameter of the inner zone is 40 cells. Outflow boundary conditions are imposed. The initial condition is:

$$\begin{aligned} (\rho, u, v, p, \gamma) &= (1, 0, 0, 1, 1.67) && \text{inner,} \\ (\rho, u, v, p, \gamma) &= (3, 0, 0, 3, 1.4) && \text{outer.} \end{aligned}$$

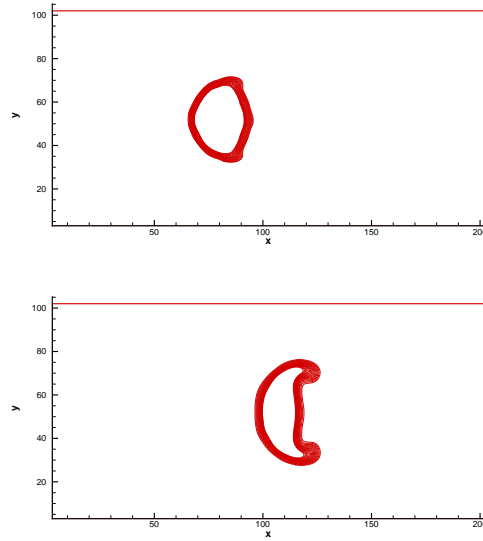


Figure 3: The first case of shock bubble interaction, the contour of density distribution is presented at time $t=50$ and $t=100$.

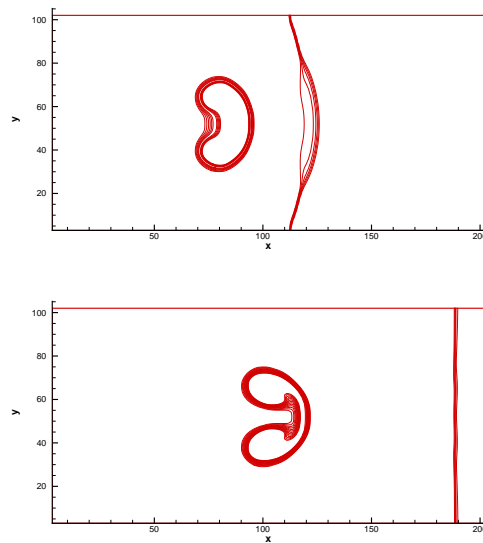


Figure 4: The second case of shock bubble interaction, the contour of density distribution is presented at time $t=100$ and $t=200$.

CFL number equals to 0.2. The numerical results of the individual densities ρ_1 and ρ_2 for each component are given at $t=15$ and $t=25$ at the fixed value $y=100$ in Fig. 5. And the total pressure profile of both species are presented at $t=10$, $t=15$, $t=20$, $t=23$ and $t=25$ in Fig. 6.

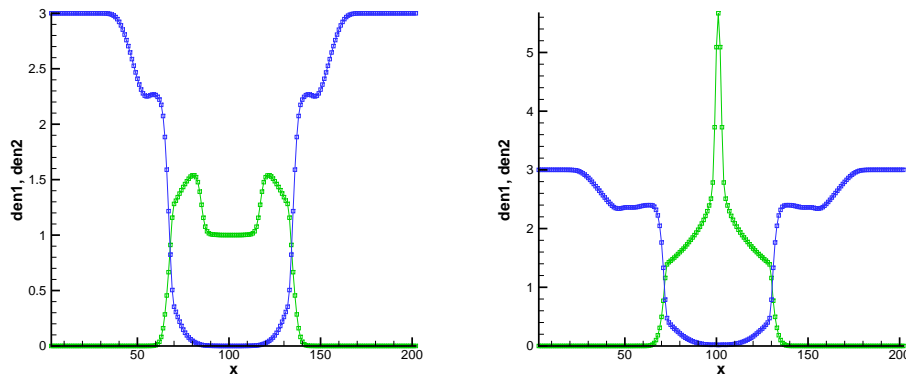


Figure 5: the density of individual mass densities ρ_1 (green), ρ_2 (blue) for each component are given at $t=15$ and $t=25$ at the fixed value $y=100$.

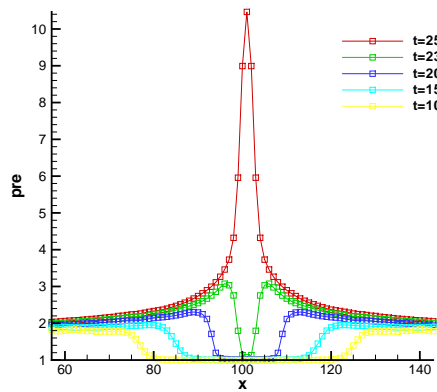


Figure 6: The contours of pressure at $t=10, t=15, t=20, t=23$ and $t=25$ at the fixed value $y=100$.

5 Numerical analysis

In the section above, the spurious oscillations of velocity and pressure were observed at the interface of two species. In this section, we analyze the reason of the spurious oscillation in the scheme proposed in the paper.

The following initial conditions with a density discontinuity evolving in uniform pressure and velocity [1] is taken into account:

$$W(x,0) = \begin{cases} (\rho_L, \rho_L U_L, \rho_L E_L), & x < 0, \\ (\rho_R, \rho_R U_R, \rho_R E_R), & x > 0, \end{cases}$$

where $\rho_L \neq \rho_R, \gamma_L \neq \gamma_R, U_L = U_R = const, p_L = p_R = const$. The exact solution of pressure and velocity is constant. $x = x_{k+1/2}$ is set as the interface of the two species. This initial

condition can be converted into the following form:

$$U_{1,j}^n = \begin{cases} (\rho_{1,j}^n, U_0, P_0), & j \leq k, \\ (\rho_{1,j}^n, U_0, 0), & j > k, \end{cases} \quad U_{2,j}^n = \begin{cases} (\rho_{2,j}^n, U_0, 0), & j \leq k, \\ (\rho_{2,j}^n, U_0, P_0), & j > k. \end{cases}$$

The initial condition of velocity and pressure can be written as:

$$U_{i,k-1}^n = U_{i,k}^n = U_{i,k+1}^n = U_0 > 0, \quad i = 1, 2$$

and

$$\begin{aligned} p_{1,k-1}^n &= p_{1,k}^n = p_{2,k+1}^n = P_0, \\ p_{2,k-1}^n &= p_{2,k}^n = p_{1,k+1}^n = 0. \end{aligned}$$

In the presented scheme, the method of operator splitting is used. It is observed that the ordinary equation part does not exert influence on the distribution of average velocity and total pressure in the next step. In consequence, we only need to focus on the hyperbolic part, i.e.

$$W_{i,k}^{n+1} = W_{i,k}^n - \sigma(F_{i,k+1/2}^n - F_{i,k-1/2}^n), \tag{5.1}$$

where $\sigma = \frac{\Delta t}{\Delta x}$.

However, the gas distribution function f_i is very complex and it is difficult to analyze the reason of spurious oscillations based on BGK scheme. So, for the sake of simplicity, the gas distribution functions could be simplified into the following KFVS form:

$$f_{i,k+1/2} = g_{i,k}^n H(u) + g_{i,k+1}^n (1 - H(u)). \tag{5.2}$$

The moments of u in the half space are denoted as:

$$\begin{aligned} \rho_{i,k}^n \langle \dots \rangle_{k,+}^i &= \int_{u>0} \int (\dots) g_{i,k}^n du d\zeta_i, \\ \rho_{i,k}^n \langle \dots \rangle_{k,-}^i &= \int_{u<0} \int (\dots) g_{i,k}^n du d\zeta_i. \end{aligned}$$

Substituting (5.2) into the density equation of (5.1), and making use of the moment relation, we can obtain the density equation:

$$\begin{aligned} \rho_{i,k}^{n+1} &= \rho_{i,k}^n - \sigma(F_{i,k+1/2}^{n,M} - F_{i,k-1/2}^{n,M}) \\ &= \rho_{i,k}^n - \sigma \left(\rho_{i,k}^n \langle u^1 \rangle_{k,+}^i + \rho_{i,k+1}^n \langle u^1 \rangle_{k+1,-}^i - \rho_{i,k-1}^n \langle u^1 \rangle_{k-1,+}^i - \rho_{i,k}^n \langle u^1 \rangle_{k,-}^i \right). \end{aligned} \tag{5.3}$$

In order to obtain an exact solution of this problem, the value of $\rho_{i,k}^{n+1}$ is assumed to be exact in the following discussion.

For the momentum equation, we also make use of the moment relationship [24] and the initial conditions, the momentum equation can be written as:

$$\begin{aligned} \rho_{i,k}^{n+1} U_{i,k}^{n+1} &= \rho_{i,k}^n U_{i,k}^n - \sigma (F_{i,k+1/2}^{n,P} - F_{i,k-1/2}^{n,P}) \\ &= \rho_{i,k}^n U_{i,k}^n - \sigma \left(\rho_{i,k}^n \langle u^2 \rangle_{k,+}^i + \rho_{i,k+1}^n \langle u^2 \rangle_{k+1,-}^i - \rho_{i,k-1}^n \langle u^2 \rangle_{k-1,+}^i - \rho_{i,k}^n \langle u^2 \rangle_{k,-}^i \right) \\ &= U_0 \left(\rho_{i,k}^n - \sigma \left(\rho_{i,k}^n \langle u^1 \rangle_{k,+}^i + \rho_{i,k+1}^n \langle u^1 \rangle_{k+1,-}^i - \rho_{i,k-1}^n \langle u^1 \rangle_{k-1,+}^i - \rho_{i,k}^n \langle u^1 \rangle_{k,-}^i \right) \right) \\ &\quad + \sigma \left(p_{i,k}^n \langle u^0 \rangle_{k,+}^i + p_{i,k+1}^n \langle u^0 \rangle_{k+1,-}^i - p_{i,k-1}^n \langle u^0 \rangle_{k-1,+}^i - p_{i,k}^n \langle u^0 \rangle_{k,-}^i \right). \end{aligned}$$

Substituting $\rho_{i,k}^{n+1} U_{i,k}^{n+1}$ into the definition of average velocity, and making use of the initial condition, the average velocity U_k^{n+1} can be simplified as:

$$\begin{aligned} U_k^{n+1} &= \frac{\rho_{1,k}^{n+1} U_{1,k}^{n+1} + \rho_{2,k}^{n+1} U_{2,k}^{n+1}}{\rho_{1,k}^{n+1} + \rho_{2,k}^{n+1}} \\ &= U_0 + \sigma \frac{P_0}{\rho_{1,k}^{n+1} + \rho_{2,k}^{n+1}} \left(\langle u^0 \rangle_{k,+}^i + \langle u^0 \rangle_{k+1,-}^i - \langle u^0 \rangle_{k-1,+}^i - \langle u^0 \rangle_{k,-}^i \right). \end{aligned}$$

In order to satisfy the exact solution $U_k^{n+1} = U_0$, we must have the following condition satisfied:

$$\epsilon_0 = \langle u^0 \rangle_{k,+}^1 + \langle u^0 \rangle_{k+1,-}^2 - \langle u^0 \rangle_{k-1,+}^1 - \langle u^0 \rangle_{k,-}^1 = 0. \tag{5.4}$$

If the exact solution of average velocity is satisfied, we take the energy equation into account. Similarly, according to the moment relationship, and for simplicity, denote $\Gamma_i = \frac{1}{\gamma_i - 1} + \frac{1}{2}$, the energy equation can be written into the following form:

$$\begin{aligned} \rho_{i,k}^{n+1} E_{i,k}^{n+1} &= \frac{1}{2} \rho_{i,k}^n U_0^2 + \frac{p_{i,k}^n}{\gamma_i - 1} \\ &\quad - \frac{1}{2} \sigma U_0^2 \left(\rho_{i,k}^n \langle u^0 \rangle_{k,+}^i + \rho_{i,k+1}^n \langle u^0 \rangle_{k+1,-}^i - \rho_{i,k-1}^n \langle u^0 \rangle_{k-1,+}^i - \rho_{i,k}^n \langle u^0 \rangle_{k,-}^i \right) \\ &\quad - \sigma \Gamma_i \left(p_{i,k}^n \langle u^1 \rangle_{k,+}^i + p_{i,k+1}^n \langle u^1 \rangle_{k+1,-}^i - p_{i,k-1}^n \langle u^1 \rangle_{k-1,+}^i - p_{i,k}^n \langle u^1 \rangle_{k,-}^i \right) \\ &\quad + \frac{1}{2} \sigma U_0 \left(p_{i,k}^n \langle u^0 \rangle_{k,+}^i + p_{i,k+1}^n \langle u^0 \rangle_{k+1,-}^i - p_{i,k-1}^n \langle u^0 \rangle_{k-1,+}^i - p_{i,k}^n \langle u^0 \rangle_{k,-}^i \right). \end{aligned}$$

By making use of the initial condition, $\sum_{i=1}^2 \rho_{i,k}^{n+1} E_{i,k}^{n+1}$ can be simplified as:

$$\begin{aligned} \sum_{i=1}^2 \rho_{i,k}^{n+1} E_{i,k}^{n+1} &= \sum_{i=1}^2 \left(\frac{1}{2} U_0^2 \rho_{i,k}^{n+1} + \frac{p_{i,k}^n}{\gamma_i - 1} \right) \\ &\quad + \frac{1}{2} \sigma U_0 P_0 \left(\langle u^0 \rangle_{k,+}^1 + \langle u^0 \rangle_{k+1,-}^2 - \langle u^0 \rangle_{k-1,+}^1 - \langle u^0 \rangle_{k,-}^1 \right) \\ &\quad - \sigma P_0 \left(\Gamma_1 \langle u^1 \rangle_{k,+}^1 + \Gamma_2 \langle u^1 \rangle_{k+1,-}^2 - \Gamma_1 \langle u^1 \rangle_{k-1,+}^1 - \Gamma_1 \langle u^1 \rangle_{k,-}^1 \right). \end{aligned}$$

Because $U_k^n = U_0 > 0$, the exact solution in the k -th cell must satisfy $p_{1,k}^{n+1} = P_0$ and $p_{2,k}^{n+1} = 0$. In order to guarantee the exact solution in the $n+1$ -th level and the energy conservation for the whole system, the following condition should also be satisfied:

$$\epsilon_1 = \Gamma_1 \langle u^1 \rangle_{k,+}^1 + \Gamma_2 \langle u^1 \rangle_{k+1,-}^2 - \Gamma_1 \langle u^1 \rangle_{k-1,+}^1 - \Gamma_1 \langle u^1 \rangle_{k,-}^1 = 0. \quad (5.5)$$

Thus, from the discussion above, in order to satisfy the exact solution of the initial condition, the following so-called moment conditions should be guaranteed:

$$\begin{aligned} \epsilon_0 &= \langle u^0 \rangle_{k,+}^1 + \langle u^0 \rangle_{k+1,-}^2 - \langle u^0 \rangle_{k-1,+}^1 - \langle u^0 \rangle_{k,-}^1 = 0, \\ \epsilon_1 &= \Gamma_1 \langle u^1 \rangle_{k,+}^1 + \Gamma_2 \langle u^1 \rangle_{k+1,-}^2 - \Gamma_1 \langle u^1 \rangle_{k-1,+}^1 - \Gamma_1 \langle u^1 \rangle_{k,-}^1 = 0. \end{aligned}$$

However, in most cases, it is difficult to satisfy the two conditions. Once one of these two conditions are violated, the spurious oscillation of velocity and pressure could be observed. It is the reason that generates the spurious oscillations at the interface.

Although the moment conditions are only based on the simplified form of our scheme, they will still become important criterions to construct gas kinetic schemes for the multi-component flow in the future.

6 Conclusion

In this paper, a new gas-kinetic scheme based on the two-species BGK model for the compressible multicomponent flows is presented. In two-species BGK model, both species are treated separately. In consequence, compared with other methods [8, 19, 26] for the compressible multicomponent flows, it is possible for us to obtain the information of each species. Different from the previous BGK schemes for the multicomponent flow, the collisions both between the same species and different species were taken into account. Based on the Chapman-Enskog expansion, the macroscopic governing equations corresponding to this model were derived. It is proved that the two-species BGK model satisfies the entropy condition. Based on this model, we constructed the numerical scheme. Because of the presence of the relaxation terms, the method of operator splitting is used. In the hyperbolic part, the numerical flux is obtained by taking moments of the gas distribution functions at the interface, which is obtained from the integral solution of the BGK equation. Numerical experiments are presented in this paper to validate the current approach in one and two dimensional cases. The numerical results are in good agreement with other numerical schemes [8, 9, 15, 26] and the experiments [17]. However, in the numerical test, the spurious oscillations were observed at the interface of the two species in the contour of velocity and pressure. We analyze the reason of the spurious oscillations and obtain the so-called moment conditions. Once these two conditions are violated, the oscillations will appear at the interface.

Acknowledgments

This work was supported by Natural Science Foundation of China (NSFC) No. 10931004, No. 11171037 and No. 91130021. The author would like to thank Professor Guoxi Ni for his useful suggestion.

References

- [1] R. Abgrall, How to prevent pressure oscillations in multicomponent flow calculations, Quasi conservative approach. *J. Comput. Phys.* 125 (1996) 150-160.
- [2] R. Abgrall and S. Karni, Computations of compressible multifluids, *J. Comput. Phys.* 169 (2001) 594-623.
- [3] P.L. Bhatnagar, E.P. Gross, M. Krook, A Model for Collision Processes in Gases I: Small Amplitude Processes in Charged and Neutral One-Component Systems, *Phys. Rev.* 94 (1954) 511-525.
- [4] C. Cercignani, *The Boltzmann Equation and its Applications*, Springer-Verlag, (1988).
- [5] S. Chapman, T.G. Cowling, *The Mathematical theory of Non-Uniform Gases*, third edition, Cambridge University Press, (1990).
- [6] R.P. Fedkiw, T. Aslam, B. Merriman, S. Osher, A non-oscillatory Eulerian approach to interfaces in multimaterial flows (the Ghost Fluid Method), *J. Comput. Phys.* 152 (1999) 457-492.
- [7] J.F. Haas, B. Strurtevant, Interactions of a shock waves with cylindrical and spherical gas inhomogeneities. *Journal of Fluids Mechanics.* 181 (1987) 41-76.
- [8] S. Jiang, G.X. Ni, A γ -model BGK scheme for compressible multifluids, *Int. J. Numer. Meth. Fluid* 46 (2004) 163-182
- [9] S. Jiang, G.X. Ni, A second order γ -model BGK scheme for multifluids compressible flows. *Applied numerical mathematics* 57 (2007) 597-608.
- [10] A.D. Kotelnikov, D.C. Montgomery, A Kinetic Method for Computing Inhomogeneous Fluid Behavior, *J. Comput. Phys.* 134 (1997) 364-388.
- [11] S. Karni, Multicomponent flow calculations by a consistent primitive algorithm, *J. Comput. Phys* 128 (1994) 237-253.
- [12] S. Karni, Hybrid multifluid algorithms, *SIAM J. Sci. Comput.* 17 (1996) 1019.
- [13] B. Larrouturou, How to Preserve the Mass Fraction Positive When Computing Compressible Multi-component Flow, *J. Comput. Phys.* 95 (1991) 59-84.
- [14] Q. Li, K. Xu, S. Fu, A High-order Gas-Kinetic Navier-Stokes flow solver, *J. Comput. Phys.* 229 (2010) 6715-6731.
- [15] Y.S. Lian, K. Xu, A Gas-Kinetic Scheme for Multimaterial Flows and Its Application in Chemical Reactions. *J. Comput. Phys.* 163 (2000) 349-375.
- [16] S. Osher, R.P. Fedkiw, Level set methods: An overview and some recent results, *J. Comput. Phys.* 169 (2001) 463-502.
- [17] J.J. Quirk, S. Karni, On the dynamics of a shock bubble interaction, *J. Fluid Mech.* 318 (1996) 129-163.
- [18] P.L. Roe, A new approach to computing discontinuous flow of several ideal gases, Technical Report, Cranfield Institute of Technology. 1984.
- [19] K.M. Shyue, An efficient shock-capturing algorithm for compressible multicomponent problems, *J. Comput. Phys.* 142 (1998) 208-242.

- [20] K.M. Shyue, A fluid-mixture type algorithm for compressible multicomponent flow with Mie-Grueisen equation of state, *J. Comput. Phys.* 171 (2001) 678-707.
- [21] R. Saurel, R. Abgrall, A simple method for compressible multifluid flows, *SIAM J. Sci. Comput.* 21 (1999) 1115-1145.
- [22] R. Saurel, R. Abgrall, A multiphase Godunov method for compressible multifluid and multiphase flows, *J. Comput. Phys.* 150 (1999) 425-467.
- [23] H.Z. Tang, K. Xu, A high-order gas-kinetic method for multidimensional ideal magnetohydrodynamics. *J. Comput. Phys.* 165 (2000) 69-88
- [24] K. Xu, Gas kinetic schemes for unsteady compressible flow simulations, *Lecture Note Ser.*,1998-03, Von Karman Institute for Fluid Dynamics Lecture. 1998.
- [25] K. Xu, A gas-kinetic BGK scheme for the Navier–Stokes equations and its connection with artificial dissipation and Godunov method, *J. Comput. Phys.* 171 (2001) 289-335.
- [26] K. Xu, BGK-based scheme for multicomponent flow calculations, *J. Comput. Phys.* 134 (1997) 122-133.
- [27] K. Xu, Discontinuous Galerkin BGK method for viscous flow equations: one-dimensional systems, *SIAM J. Sci. Comput.* 23 (2004) 1941-1963.
- [28] K. Xu, Gas-kinetic theory based flux splitting method for ideal magnetohydrodynamics, *J. Comput. Phys.* 153 (1999) 344-375
- [29] K. Xu, J.C. Huang, A unified gas-kinetic scheme for continuum and rarefied flows *J. Comput. Phys.* 229 (2010), 7747-7764.
- [30] K. Xu, A Well-Balanced Gas-Kinetic Scheme for the Shallow-Water Equations with Source Terms, *J. Comput. Phys.* 178 (2002) 533-562.
- [31] R. Samtaney, N.J. Zabusky, Circulation deposition on shock-accelerated planar and curved density-stratified interfaces: models and scaling laws, *J. Fluid Mechanics*, 269, (1994), 45-78.